SONIC CRYSTALS, METASURFACES, ACOUSTIC INVISIBILITY AND BLACK HOLES

K Attenborough Engineering and Innovation, The Open University, Milton Keynes, UK
Y B A Chong TWI, Granta Park, Great Abington, Cambridge CB21 6AL, UK
I Bashir Department of Renewable Energy, University of Exeter, Cornwall Campus, UK.
H-C Shin Engineering and Innovation, The Open University, Milton Keynes, UK
S Taherzadeh Engineering and Innovation, The Open University, Milton Keynes, UK

1 INTRODUCTION

Materials with properties not found in natural or continuous media can be designed by using artificial, often periodically-spaced, sub-units. The acoustical properties of many materials can be characterised by their effective density and elastic moduli. In conventional lossy materials these quantities are complex with positive real parts. In periodicity-enhanced materials, often called *metamaterials*, the effective density and elastic moduli can attain negative values. The metamaterial does not support 'forward' propagating waves in ranges of frequencies in which either of these quantities is negative, and there is a “stop band”. A stop band is complete if it applies at all angles of incidence. Within a complete stop band, a finite size structure reflects back nearly all incident sound irrespective of the incidence angle thereby allowing very little transmission through it. If both effective properties are negative, a metamaterial exhibits negative refraction[1]. Although there have been extensive studies and developments relating to *photonic* metamaterials i.e. materials which can mould the flow of light under certain conditions, comparatively little effort has been expended in respect of materials that can alter the distribution of sound energy (i.e. phononic metamaterials).

A phononic or sonic crystal (SC) consists of regular 2D arrays of solid cylinders in a host material, which can be either another solid or a fluid such as air with contrasting acoustical properties. Multiple scattering by the cylindrical inclusions at wavelengths similar to the cylinder radius and spacing gives rise to reduced transmission at some frequencies (stop bands) and enhanced transmission (focussing) at other frequencies (pass bands) depending upon the centre-to-centre spacing of the cylinders (the lattice constant). The amplitudes of the stop and pass bands depend on the fraction of the total volume of the array occupied by scatterers which is known as the filling fraction. The filling fraction depends on the lattice constant and the cylinder radius. Below the first stop band frequency, arrays of solid cylinders in a fluid may be modelled as effective fluids in which the effective sound speed depends on the lattice constant and filling fraction.

At wavelengths much larger than the embedded sub-units, metamaterials such as sonic crystals in air, may be regarded as effective fluids with frequency dependent properties. Some types of metamaterials involve graded effective properties by varying both the properties of the sub-wavelength scatterers and their filling fractions. Example applications include a gradient acoustic lens[2] and a magnifying lens[3]. Also it has been shown that by surrounding an object by a highly anisotropic metamaterial layer, it can be made “invisible” or 'cloaked'. The waves are guided around the shielded object without scattering or the formation of a diffracted shadow beyond the ‘cloaking’ structure[4]. A particular kind of graded system incorporates a gradual power-law-type decrease in the velocity of the incident wave with propagation distance to almost zero accompanied by efficient energy absorption in the area of low wave velocity[5-7]. This is the basis of ‘black hole’ devices.

Much previous research has investigated the theoretical foundations of metamaterial behaviour and practical realisations or applications of metamaterials have been scarce. Moreover the majority of investigations of acoustical applications have centred on cloaking. Few potential applications for noise and vibration control have been investigated. The frequency dependence of the transmission loss of sonic crystals containing only rigid elements is too irregular and incident angle dependent to

be useful for controlling broadband noise. However, the performance of sonic crystal noise barriers can be improved through use of sound absorbing coverings or cores, resonant elements and optimised configurations. The latter may involve aperiodicity, vacancies and fractal arrangements. Similar approaches can be used to design a periodic surface that produces a ground effect useful for noise control and such surfaces may be called metasurfaces. After outlining the basic physical principles, this paper reviews recent developments concerning metamaterials and metasurfaces aimed at noise and vibration control. The applications explored in detail are sonic crystal acoustic barriers and the modification of acoustically-hard surfaces (metasurfaces) to reduce traffic noise. References to acoustic cloaking, although made as part of the review function of the paper, are incidental to these main emphases.

2 SONIC CRYSTAL NOISE BARRIERS

2.1 Bragg diffraction

When a plane wave is incident in air at angle θ with respect to the normal on a regular arrangement of solid elements at wavelengths comparable with the element cross sections and their spacing it undergoes multiple scattering. Scattering by regular arrangements of scatterers was first studied in the context of electromagnetic waves and is known as Bragg scattering. Consider a plane wave at angle θ to the axes of two rows of cylindrical scatterers in a rectangular array simultaneously incident on a particular cylinder in the first row and the corresponding cylinder in the second row. The distance between the wavefronts at that moment is $a\sin\theta$. If the incident wavelength is denoted by λ and the spacing by a (see Figure 1), then the condition for constructive interference between forward scattered (i.e. transmitted) waves is that $\lambda = a\sin\theta$ and this determines the frequency of the first *pass band*. At normal incidence the first pass band frequency is given by c/a. Similarly the condition for the first destructive interference is that $\lambda/2 = a\sin\theta$.
At normal incidence, this implies a first *stop band* or Bragg frequency of

$$f_{Bragg} = c/2a \qquad (1).$$

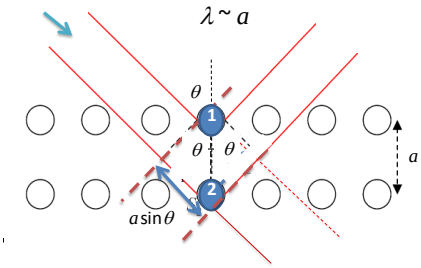

Figure 1 Multiple forward scattering of plane sound waves by two cylinders in a two-row array of regularly-spaced cylinders

As well as the behaviour at normal incidence there is interest in the behaviour along axes of symmetry (the diagonals in the case of a square lattice - see Figure 2(a)).

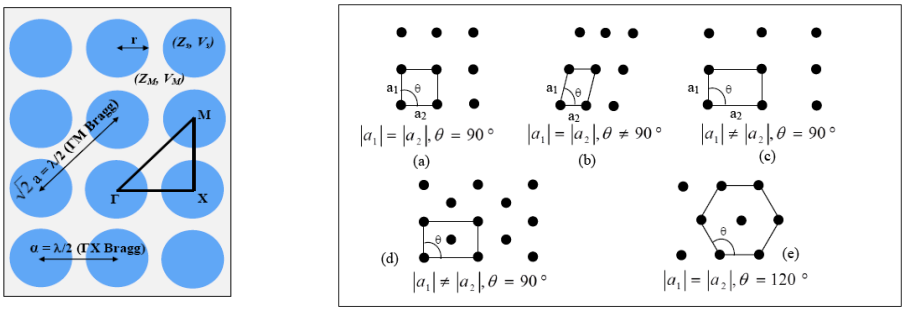

Figure 2 (a) Symmetry directions in a square array (b) Bravais lattices

Regular arrangements other than square arrays may be used for sonic crystals. Such arrangements include oblique, centred rectangular and centred hexagonal - see Figure2(b). These 5 unique 2D (Bravais) lattices are invariant in translation and rotation. As well as the lattice constant, the filling fraction (*ff*) is important since it determines the width and depth of the pass and stop bands. If the scatterer radius is denoted by r, and the lattice constant by a, then for a square array, $ff_{square} = \frac{\pi r^2}{a^2}$ and, for a hexagonal array, $ff_{hexgonal} = \frac{2\pi r^2}{\sqrt{3}a^2}$.

2.2 Results of measurements and predictions for rigid cylinders

Figure 3 shows laboratory data obtained for insertion loss due to a 7×3 array of PVC pipes with outer diameter 5.5 cm with lattice constants of 0.069 m and 0.135 m corresponding to filling fractions of 0.5 and 0.13 respectively. Using $f_{Bragg} = c/2a$, these lattice constants correspond to first Bragg frequencies at 2.49 kHz and 1.35 kHz respectively. The smaller filling fraction results in the first stop band having a lower amplitude than the second. Also shown are predictions of multiple scattering theory assuming plane waves and a cylindrical line source respectively. For the laboratory geometry, both predictions are comparably accurate.

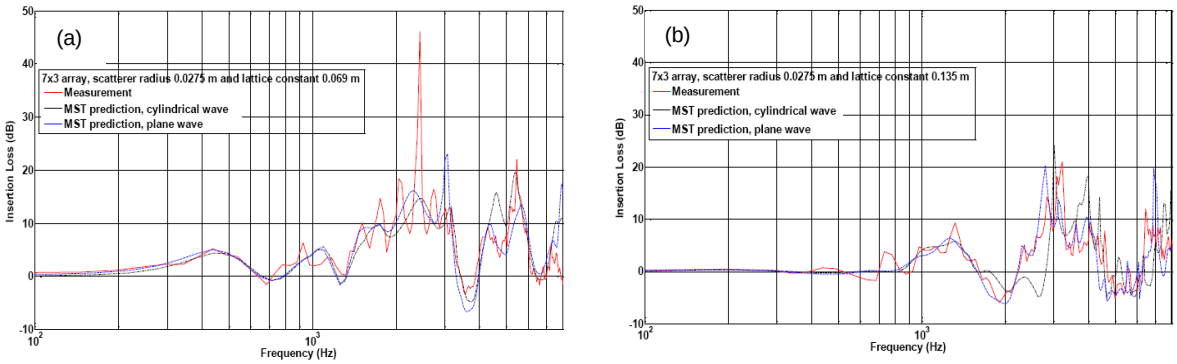

Figure 3 Laboratory data obtained for the insertion loss of a 7x3 square lattice arrays of PVC pipes of OD 5.5 cm with lattice constants of (a) 0.069 m and (b) 0.135 m compared with predictions of Multiple Scattering Theory (MST) assuming either cylindrical waves or plane waves incident[8].

Figure 4(a) shows a sonic crystal barrier composed from three rows of 54 (11 cm OD) PVC pipes with a lattice constant of 16 cm 'sandwiched' between two regular wooden noise barrier panels at the Open University Barrier Test Site. Figure 4(b) shows the arrangement for making insertion loss (IL) measurements as a function of angle[8]. Figure 5 shows example IL data and predictions.

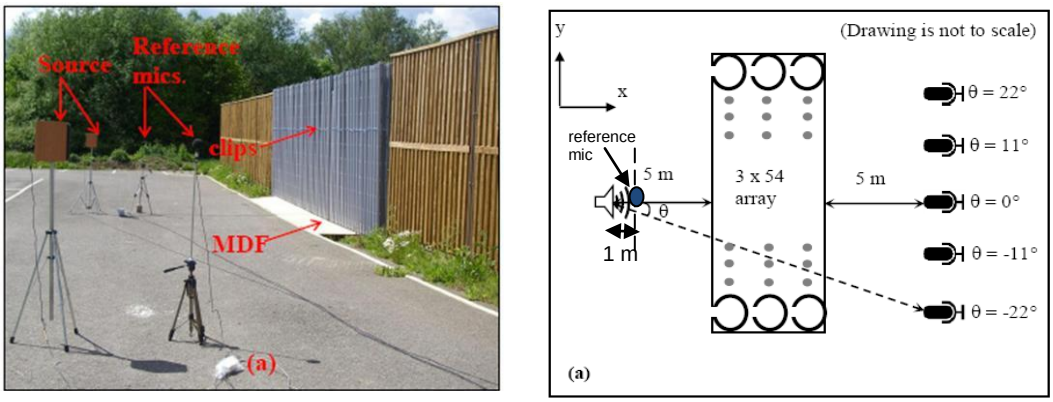

Figure 4 (a) Sonic crystal barrier composed from 3m long 11 cm OD PVC pipes at the OU barrier test site (b) arrangement for measuring insertion loss.

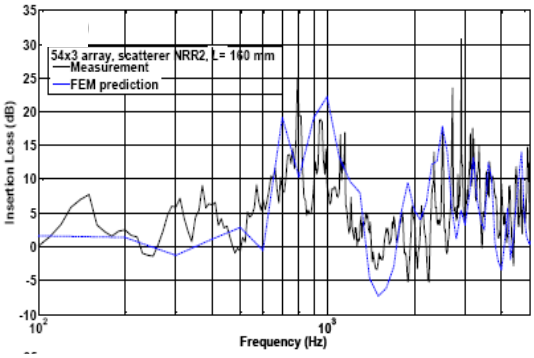

Figure 5 Measured and predicted (FEM) insertion loss of a 54×3 outdoor square array (lattice constant 16 cm corresponding to f_{Bragg} = 1 kHz) of PVC pipes at normal incidence.

The predictions are made using a Finite Element Method (FEM) code COMSOL®. Insertion loss spectra such as those shown in Figures 3 and 5 are typical of those resulting from transmission through regularly-spaced rigid cylinder arrays. They are too frequency (and angle) dependent to be useful for surface transport noise control. However there are several ways of improving the insertion loss of sonic crystal noise barriers. These include adding absorption, making the sub-units resonant and optimising the array configuration. Examples of these methods are reported in the sections 2.3 to 2.6.

2.3 Effects of adding absorption

Figure 6(a) shows insertion loss data obtained in a laboratory on a 7×3 array of 0.953 cm diameter 2m long aluminium rods, lattice constant 1.5 cm (f_{Bragg} = 11.4 kHz), without and with 0.175 m thick felt coverings using an acoustic spark source with peak energy near 15 kHz at 1.5 m from the source (i.e. at the front row of the array)[9]. The added absorption reduces the pass bands while increasing the insertion loss at higher frequencies. Figure 6(b) shows predictions of multiple scattering theory[9] (MST) which suggest that the thickness of the absorptive covering can be optimised. In this small scale laboratory configuration, the optimum thickness is near 0.17 cm.

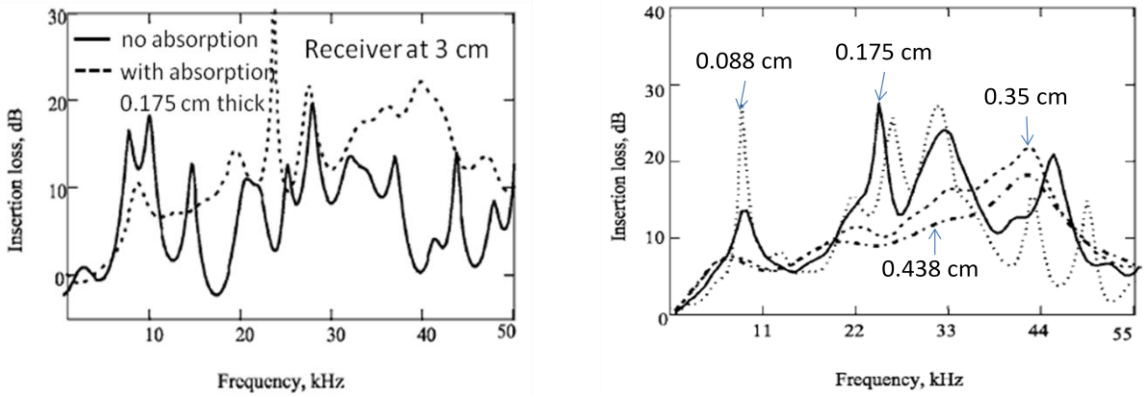

Figure 6 (a) Insertion loss data obtained at 3 cm from the edge of a 7×3 square array (1.5 cm lattice constant) of 2 m long aluminium cylinders (without and with 0.175 cm thick felt covering) furthest from a spark source located at 1.5 m from the nearest edge of the array (b) (MST) predicted effects of changing the felt cover thickness[9].

More recent but related research has investigated the performance of larger sonic crystal arrays composed from porous cylinders protected by thin outer perforated metal shells[10]. The porous cylinders were made from rubber crumb recycled from car tyres. MST predictions were found to agree with measurements on 9×3 square arrays (11 cm lattice constant) of 1m long 8 cm OD porous cylinders with wall thicknesses between 2 and 4 cm and. Both predictions and data showed large stop bands near 1.5 and 3 kHz.

2.4 Locally-Resonant Sonic Crystals

2.4.1 Slit Cylinders

Insertion loss peaks below the first Bragg stop band can be obtained by making the sub-units resonate at an appropriate frequency. An array of regularly spaced resonant elements is known as a locally-resonant sonic crystal. The 11 cm OD PVC pipes mentioned previously have been made resonant by creating a row of approximately 12 mm wide and 30 cm long slots (see the inset photograph in Figure 7(b)) along each of them[8]. This has the effect of introducing a resonance at about 450 Hz (compare Figs.7(a) and (b)) in the insertion loss due to a single cylinder, which is strongest when the slots face the source (see Figures 7(c) and (d)).

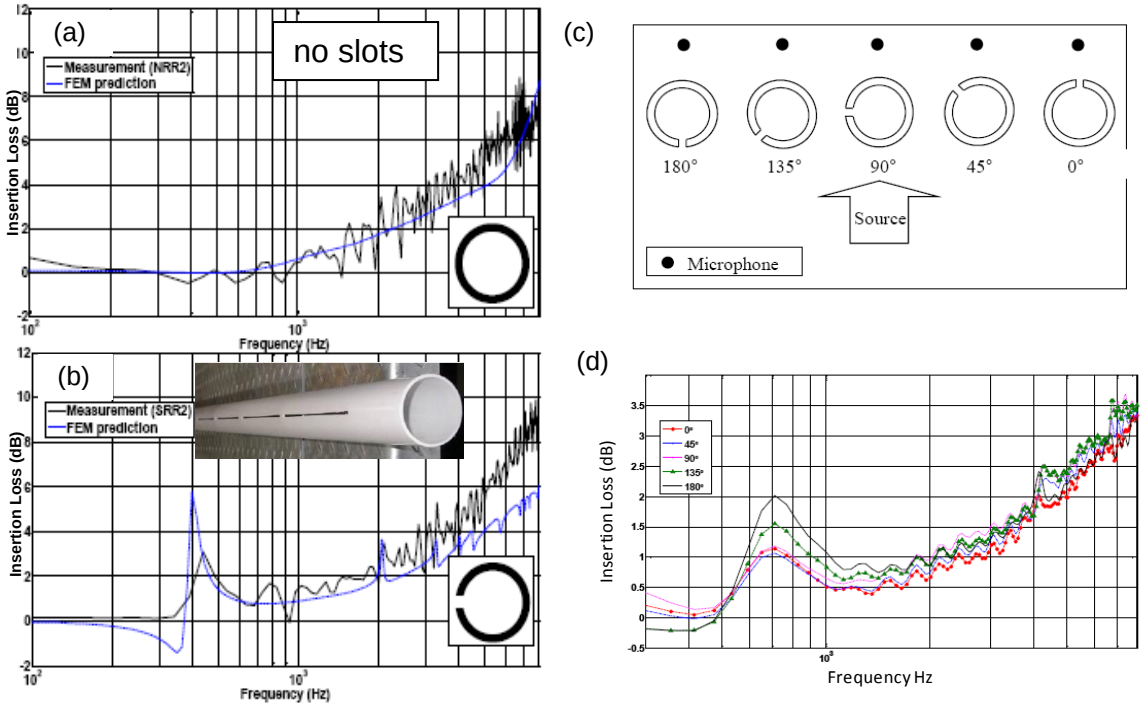

Figure 7 Insertion loss (IL) spectra measured and predicted (Finite Element Method (FEM) COMSOL®) for single 11 cm OD PVC pipe (a) without and (b) with 12 mm wide slots (see inset in (b)) respectively at normal incidence (c) five rotations of slots with respect to source (d) IL spectra measured at these five angles of rotation[8].

Corresponding insertion loss spectra measured and predicted for the outdoor PVC pipe sonic crystal (Fig.4(a)) are shown in Figure 8.

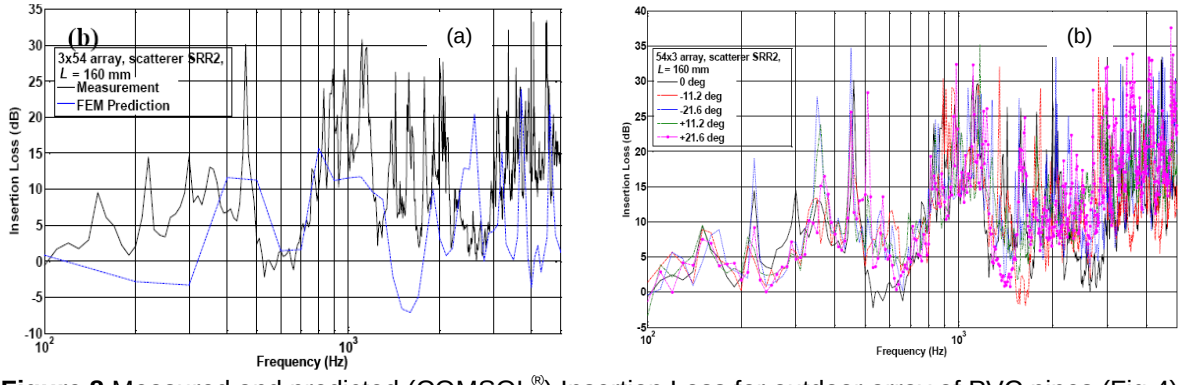

Figure 8 Measured and predicted (COMSOL®) Insertion Loss for outdoor array of PVC pipes (Fig.4) with slots (a) at normal incidence (b) measured at five azimuthal angles of incidence[8].

The 450 Hz resonance observed in the insertion loss spectrum for the single slotted cylinder is present in the insertion loss spectra for the outdoor array and is not much affected by angle of incidence.

2.5 Elastic Shell Resonators

Another type of resonant element is a thin-walled elastic shell. This makes use of the 'breathing' mode and higher modes of shell vibration. Sonic crystals composed from thin-walled elastic shells have been realised in the laboratory using balloons[11,12] and from Latex® sheets formed into 5.5 cm OD cylinders, with wall thickness 0.25 mm, by overlapping and gluing opposing edges[8]. Figures 9(a) and 9(b) show measured and predicted insertion loss spectra of a single cylindrical shell and a 7×3 array (lattice constant 8 cm) of shells[8,13]. The Latex® shell cylinders have a 'breathing mode' near 1 kHz. To preserve an approximately cylindrical shapes the shells were slightly inflated.

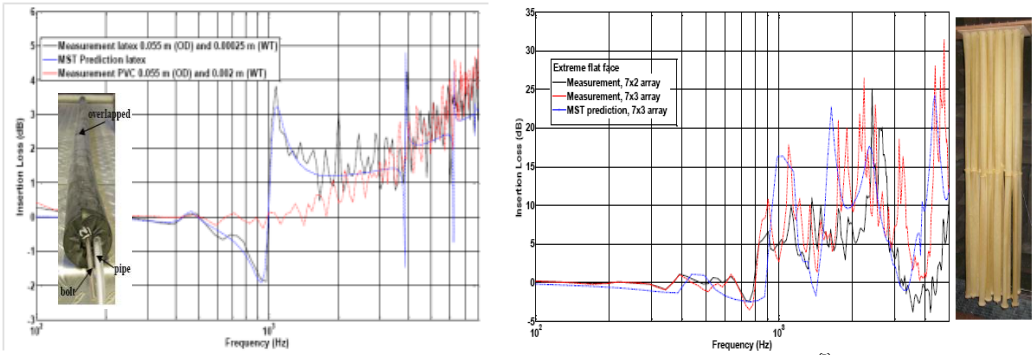

Figure 9 IL spectra measured and predicted (using MST) for a single Latex® shell (5.5 cm OD, wall thickness 0.25 mm) and 7×2 and 7×3 arrays (lattice constant 8 cm) of similar shells.

2.6 Multiple and Coupled Resonances

Additional stop bands at frequencies below the first Bragg frequency can be achieved in sonic crystals by incorporating elements with different resonant frequencies. This has been predicted numerically using 'Matroyshka' (Russian Doll) arrangements of concentric slit cylinders[14] and semi-analytically and measured in the laboratory using elements with multiple coupled resonances[8,15,16]. Figure 10(a) shows a concentric arrangement of an elastic shell and an outer rigid cylinder having four symmetrically-arranged slits to allow the breathing mode resonance of the inner elastic shell. Figure 10(b) shows laboratory insertion loss data for a single concentric arrangement and its individual components (0.043 m OD elastic shell and 0.055 m OD PVC pipe). Figure 10(c) shows laboratory insertion loss data for corresponding 7×3 arrays (lattice constant 0.08 m (f_{Bragg} = 2 kHz)[8]. The data for the composite arrangements are denoted by 'SRR3'. The IL data for the single composite cylinder and the array of composite cylinders show a modified (reduced frequency) 'breathing mode' resonance near 1 kHz and an additional resonance near the Bragg frequency related to the cavity between the inner and outer components. An interesting feature in Fig. 10(c) is the enhanced 'finite' array size effect near 750 Hz for the composite cylinder array.

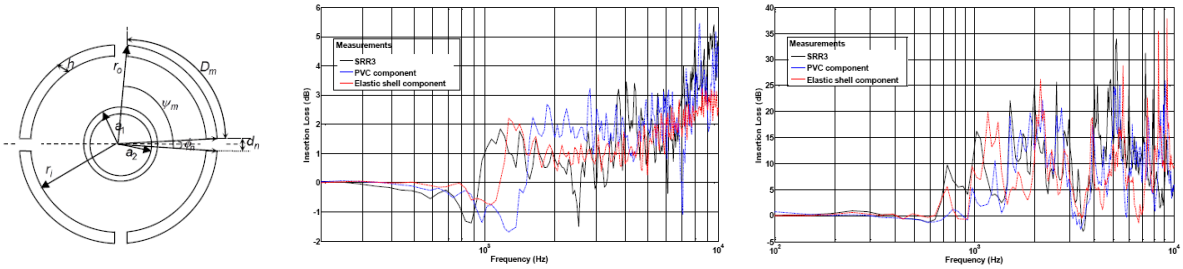

Figure 10 (a) A composite cylinder arrangement of an inner elastic shell and an outer symmetrically-slit rigid cylinder (b) insertion loss data for the composite cylinder and its components (c) insertion loss data[8] for corresponding 7×3 square arrays with lattice constant 0.08 m.

Another type of coupled resonance scatterer consists of a U-shaped formed from recycled polymer mounted on a rigid plate. The resonances in the arms of the U-shape and of the contained cavity feature in the resulting insertion loss spectra for an array of such elements below the first Bragg frequency[16]. Recent results using coupled pairs of slit cylinders are described elsewhere[17].

2.7 Configuration Effects

2.7.1 Vacancies

The removal of one or more elements from a regular array to create vacancies (point defects) can result in trapped modes at frequencies within the band gaps of the complete array which decay exponentially away from sites of the vacancies. When a wave at a frequency within the band gap range arrives at a vacancy it is surrounded by an array with the original lattice constant and being unable to transmit, is thereby trapped. Figure 11 shows the results measured and calculated around (a) single and (b) double vacancies[16]. The creation of two nearby vacancies gives rise to the possibility of symmetric and antisymmetric interactions between them at similar frequencies just above the first Bragg frequency associated with the original complete regular array.

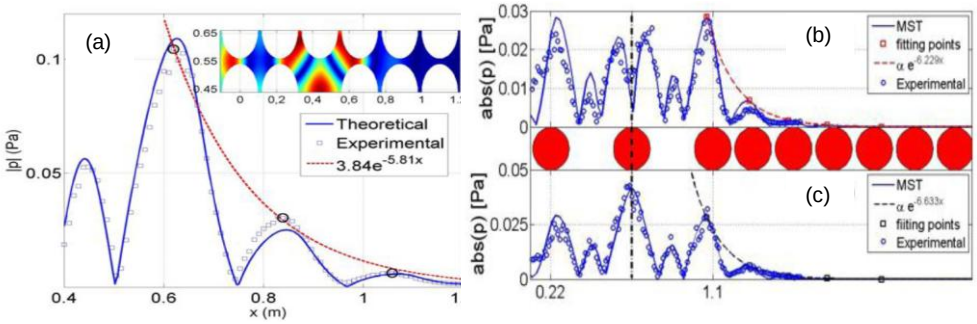

Figure 11 Measurements and predictions of the sound field inside a 6×5 square array of 0.2 m OD rigid cylinders with lattice constant 22 cm (f_{Bragg} = 780 Hz) (a) at 900 Hz around a single vacancy, showing the measured and fitted exponential decay away from the vacancy (b) at 940 Hz and (c) at 895 Hz around two neighbouring vacancies showing symmetric and anti-symmetric resonances[16].

If there are several defects within an array, then there are more complicated interactions than with a double point defect. However, as discussed in the next sub-section, they can be manipulated to give targeted insertion losses within band gaps.

2.7.2 Optimising Vacancies

The presence of several vacancies in a sonic crystal can give rise to insertion losses below the band gap frequencies[18]. The location of vacancies within a rigid cylinder array can be optimised, for example using a Genetic Algorithm, to improve the insertion loss of the 'starting' complete array in a target frequency range[16]. The resulting arrays have been called Quasi-Ordered Structures (QOS). Figure 12(a) shows a 'starting' 6×10 hexagonal array of 1 m long 4 cm OD hollow aluminium cylinders with lattice constant 6.35 cm (f_{Bragg} near 3 kHz) and the measurement arrangement. Figures 12(b) and (c) show the measured and predicted insertion loss spectra compared with that of the 'starting' array and optimised configurations for different target frequency ranges.

It has been found that the best optimisation results in terms of transmission loss are obtained when some degree of asymmetry in the distribution of vacancies is introduced. The optimal number of vacancies has been found to be around 40% of the total number of cylinders in the starting SC and the optimal asymmetry in the distributution of vacancies has been found to be near 60%.

A similar procedure can be used to produce QOS for focussing[16] but this application is not described here.

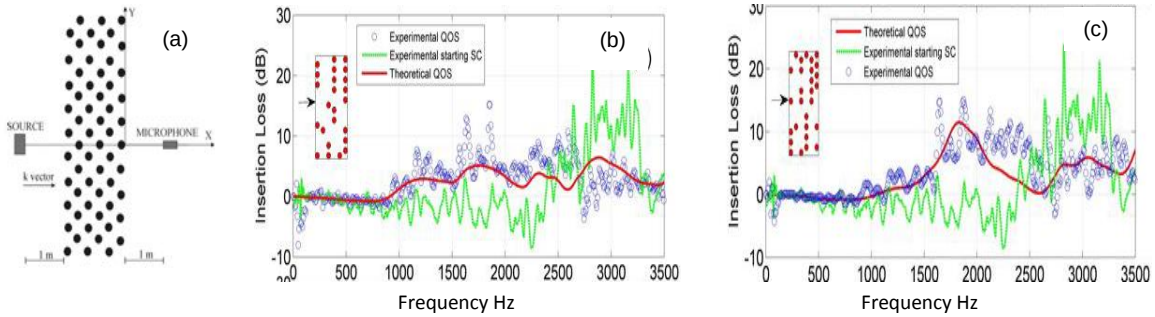

Figure 12 (a) 'starting' 6×10 hexagonal array and laboratory measurement arrangement (b) and (c) insets show array configurations optimised for improved insertion loss between 1400 and 2000 Hz and between 1700 Hz and 2300 Hz respectively with the resulting measured and predicted insertion loss spectra[16].

2.8 Absorption, resonance and fractal configuration

The results of a combination of mechanisms for improving the insertion loss of a sonic crystal including absorption, resonance and optimised configuration have been studied and measured[19]. Figure 13 shows the insertion loss spectrum predicted for an array containing two sizes of resonant (slit cylinder) elements including (internal) absorption (see insets) and two sizes of rigid cylinder in fractal arrangements. The fractal arrangement (Serpinski triangle) embeds two periodicities which result in two sets of Bragg frequencies. Also shown is the IL spectrum predicted by Maekawa's formula for a 3 m high solid barrier. The IL predictions for the composite fractal sonic crystal have been supported by transmission loss measurements[19].

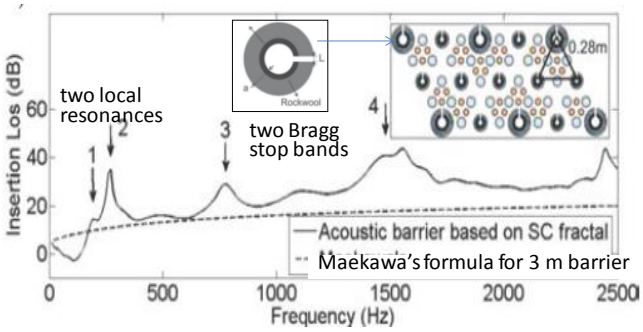

Figure 13 The construction of a fractal locally resonant sonic crystal with two sizes of resonant cylindrical elements and two sizes of solid cylinders and the predicted IL spectrum. Also shown is the Maekawa prediction for a 3 m high solid barrier[19].

2.9 Ground and Sonic Crystal Effects

So far the discussion of sonic crystal acoustic barriers has not taken into account that they must be supported on a ground surface. In the absence of the sonic crystal, the presence of a ground plane gives rise to ground effect i.e. interference between the component travelling directly to a receiver from the source and the ground-reflected component. Over 'soft' (porous) ground, and for source-receiver geometries appropriate to surface transport noise predictions, the first destructive interference gives rise to attenuation in excess of that due to wavefront spreading and air absorption and is called *ground attenuation* in standard noise prediction schemes[20]. A solid noise barrier reduces any 'soft' ground effect since it raises the effective path height for the sound. However laboratory experiments have shown that, not only is ground effect preserved in the presence of arrays of vertically-orientated cylinders, but the sonic crystal and ground effects are additive[21,22]. Figure 14 shows laboratory data obtained with source height (H_s) 0.1 m, receiver height (H_r) 0.1 m and horizontal separation (R) 1.0 m, over (a) hard ground (MDF) and (b) 'soft' ground (a 0.014 m thick layer of felt on top of MDF) without and with a 5×10 square array of 0.5 m

long 0.04 m OD PVC pipes, lattice constant 0.1 m (f_{Bragg} = 1.7 kHz, filling fraction 0.13), placed on Medium Density Fibreboard (MDF)[22].

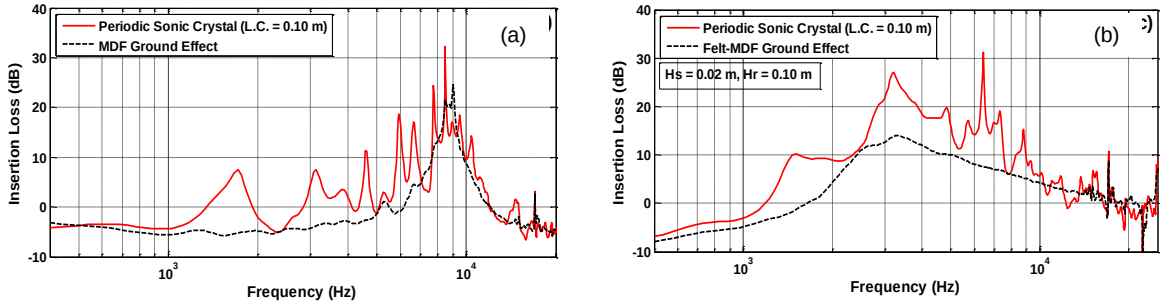

Figure 14 Measured insertion loss spectra ($H_s = H_r$ = 0.1 m, R = 1 m) over (a) 'hard' MDF and (b) 'soft' felt layer over MDF without and with a 5×10 square array of 0.5 m long 0.04 m OD PVC pipes, lattice constant 0.1 m. Also shown is the (inverted) ground effect due to each surface alone.

Without the sonic crystal array, the first destructive interference occurs at about 8 kHz. The sonic crystal array gives insertion loss peaks at the Bragg frequency (1.7 kHz) and at twice this frequency. The ground effect adds to the higher frequency insertion loss near 8 kHz. The first destructive interference over the felt layer on MDF without the sonic crystal array is broad and peaks near 3.5 kHz. The overall insertion loss spectrum is augmented by the ground effect. The combined insertion loss due to a sonic crystal composed of vertical cylinders on a horizontal ground surface can be calculated by adding the insertion loss calculated for the array (for example using MST) to the ground effect calculated for a point source over an impedance plane[21,22].

2.10 Aperiodicity effects

Measurements and predictions show that, while there is advantage for broadband sound attenuation in using a periodic sonic crystal configuration rather than one with random spacing, a quasi-periodic sonic crystal arrangement in which the perturbation has a standard deviation equal to the scatterer diameter gives the best overall attenuation[21,22]. This is illustrated by the insertion loss data in Figure 15 with source height 0.02 m, receiver height 0.1 m and separation 1 m for which the hard ground effect is near +6 dB over the frequency range shown.

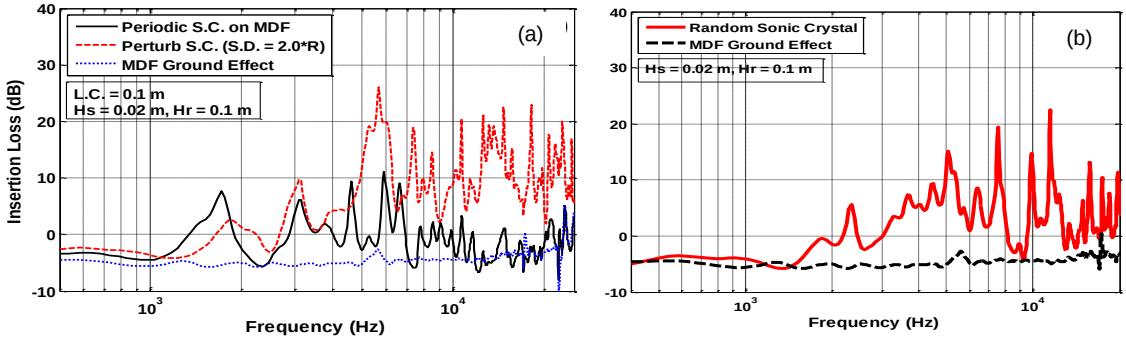

Figure 15 Measured insertion loss spectra corresponding to (a) periodic and perturbed versions of the array over MDF described for Fig.14(a) and (b) completely random versions of the array.

Fig.15(a) shows data obtained (with H_s = 0.02 m, H_r = 0.1 m, R = 1 m) for the regular array and a pseudo-random array in which the cylinder locations were perturbed by up to a diameter from their regularly-spaced locations. Also shown is MDF ground effect alone (near 6 dB for this geometry). Fig. 15(b) shows averaged data obtained for the randomly-spaced versions of the array[22].

A series of Finite Difference Time Domain calculations[23,24] have been used as the basis for an optimum tree belt design for traffic noise reduction by modelling it as a sonic crystal of tree trunks over soft ground and by using vacancies and pseudo-randomisation of trunk location and size.

3 REFRACTION AND CLOAKING WITH METAMATERIALS

At low frequencies, i.e. when one wavelength covers many periods of the structure, a regular arrangement of cylinders can be used to focus or redirect a wave which propagates through it. At such frequencies periodically spaced cylinders embedded in air behave as a modified fluid medium characterized by effective sound speed, c_{eff}, and effective density, ρ_{eff}, given by:

$$c_{eff} = \frac{c_0}{\sqrt{1+ff}}, \qquad \rho_{eff} = \frac{\rho_0\sqrt{1+ff}}{\sqrt{1-ff}}, \qquad ff < 0.6, \tag{2}$$

where ff is the filling fraction.

If the cylinder axes are horizontal and the cylinder radius or lattice spacing or both are varied then the resulting 'graded index' sonic crystal can be used as a barrier which redirects an incident wave. This idea has been used to design an upward-refracting sonic crystal noise barrier[25] in which the lattice constant is kept the same but the cylinder radius increases with height so as to simulate an upward-refracting atmospheric sound speed gradient. Figure 16(a) illustrates a scenario for calculating broadband sound reduction, with three (ground plane) source positions and three receiver zones beyond the refracting sonic crystal barrier. Fig. 16(b) shows the sound level map corresponding to 1 kHz and source position 3 (SP3 in Fig. 16(a)) and Fig. 16(c) shows the overall attenuations predicted for receiver zones 1 to 3 and a 2 m high graded index sonic crystal barrier (in which the minimum and maximum values of filling fraction and cylinder radius are $ff_{\min}$ = 0.06, $r_{\min}$ = 0.79 cm; $ff_{\max}$ = 0.28, $r_{\min}$ = 1.70 cm).

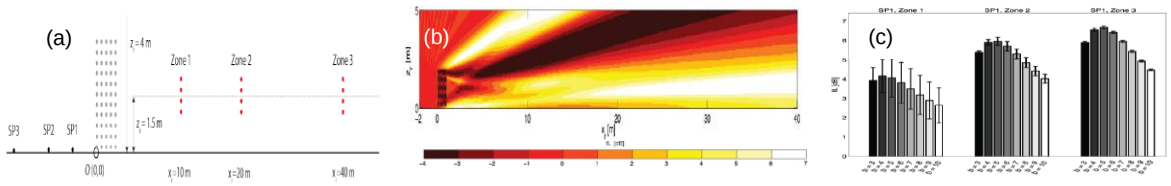

Figure 16 Predicted effects of an upward-refracting sonic crystal noise barrier[25] (a) scenario assumed for calculations (b) predicted sound level map at 1 kHz for a 2 m high graded index sonic crystal barrier (c) predicted broadband reductions in receiver zones 1 to 3.

Optimised clusters of cylinders with different local configurations have been used as the basis of a cloaking design for an airborne sound source at 3 kHz and the cloaking performance of resulting device been validated experimentally[26]. Graded Index Arrays in which the effective sound speed is reduced during propagation through the arrays and then absorbed at the reduced speed are known as 'black holes'. A design for a 'black hole' sound absorber based on graded index regularly-spaced cylinder clusters is being developed[27]. The use of a periodic array of boreholes for cloaking a building from Rayleigh waves caused by pile driving or earthquakes is being explored also[28].

4 METASURFACES FOR NOISE CONTROL

Although ground effect features in many prediction schemes there has been little work on designing ground effect for noise control. One way in which ground effect due to an acoustically-hard surface can be controlled is through the deliberate introduction of low-height (≤ 0.3 m) roughness. Figure 17 compares laboratory data for the excess attenuation due to arrays of randomly- and regularly-spaced wooden strips of various cross-sections and heights ranging between 0.008 m (semi-cylinders) and 0.0285 m (tall rectangles) placed on MDF[8,29]. The (point) source and receiver heights were 0.07 m and they were separated by 0.7 m. Randomly-spaced roughness (mean centre-to-centre spacing 0.05 m) produces a wide destructive interference band at a significantly lower frequency than that measured for the same source and receiver geometry over the MDF alone (see Fig.17(a)). When the roughness is regularly-spaced (Fig. 17(b) additional narrower diffraction-related destructive interference bands. Small scale roughness reduces the effective impedance of the smooth hard surface and this has been investigated as the basis of a method of surface

transport noise control. A particularly useful roughness for road traffic noise reduction has the form of a lattice[30].

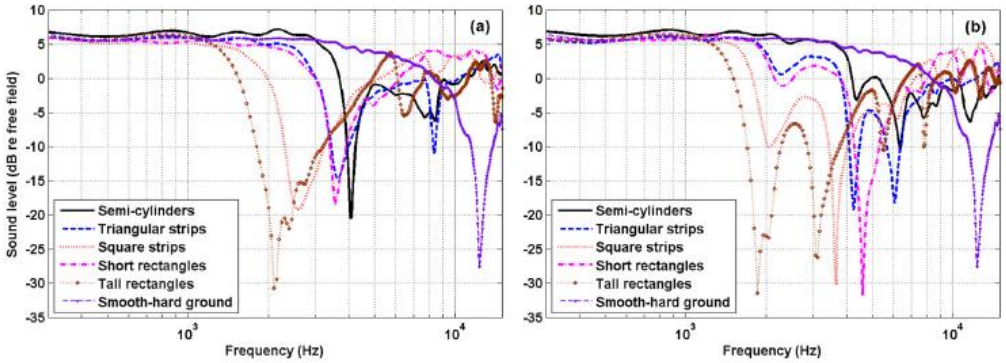

Figure 17 Excess attenuation spectra obtained with source and receiver at 0.07 m height and separated by 0.7 m over various shapes and heights of wooden strips with mean centre-to-centre spacing of 0.05 m (a) randomly distributed and (b) regularly-spaced.

Although the detailed mechanisms are different the constructive and destructive interference bands associated with ground effect due to (point) source over a plane ground may be regarded as equivalent to the pass and stop bands associated with sonic crystals and similar methods (adding absorption, resonance, optimising configuration) may be considered for improving broadband ground attenuation. Results of initial calculations and laboratory experiments to explore the potential usefulness of resonant elements[31] are shown in Figure 18 which shows plots of negative Insertion Loss (equivalent to Excess Attenuation but can be measured more accurately) obtained with (point) source height 0.08 m and receiver height 0.059 m separated by 0.95 m over an array of 9 PVC pipes with external and internal diameters of 0.055 m and 0.0526 m respectively ((a) without and (b) with slits) placed at a centre-to-centre spacing of 0.1 m on a plastic board.

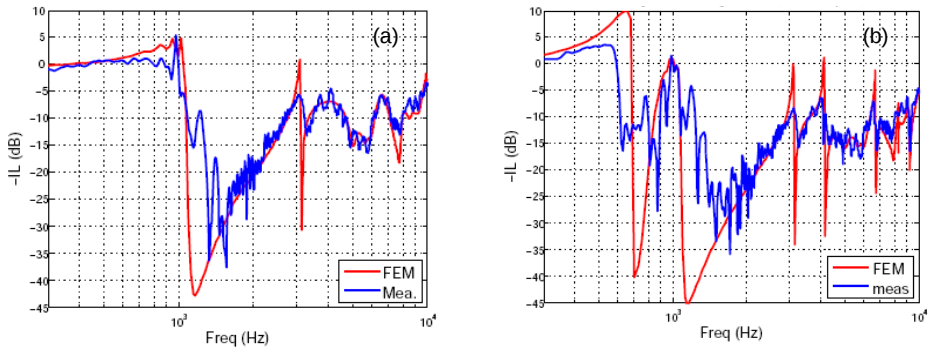

Figure 18 Insertion loss spectra measured with source height 0.08 m and receiver height 0.059 m separated by 0.95 m over an array of 9 PVC pipes with external and internal diameters of 0.055 m and 0.0526 m respectively ((a) without and (b) with slits) placed at 0.1 m centre-to-centre spacing on a plastic board. Predictions use FEM.

Also shown in Fig. 18 are numerical predictions obtained using FEM. Although the overall agreement between numerical predictions and data is reasonably good, there are discrepancies that may be due in part to the fact that the slit cylinders contained three additional rows of slits (see Fig. 10(a)) which were taped over for these experiments.

5 CONCLUDING REMARKS

Regularly-spaced arrays of rigid cylinders in air (sonic crystals) produce stop and pass bands due to Bragg diffraction, the frequencies and magnitudes of which depend on their spacing (lattice constant) and cross-section (filling fraction). To be useful as an alternative to regular noise barriers ways have to be found to make the insertion loss less frequency and angle dependent. The

insertion loss of sonic crystal barriers can be improved by adding absorption, incorporating resonant elements and by optimising array configuration. For filling fractions of 0.5 and less sonic crystal and ground effects are additive. Although the use of coupled resonator elements seems promising, more work on this method is needed. Moreover simultaneous applications of all known techniques for improvement are yet to be tried.

At frequencies below the first stop band, and by varying cylinder radius or lattice constants or both, clusters of regularly-spaced cylinders can be used to produce upward-refracting noise barriers, graded index absorbers, and acoustic cloaks.

Small scale roughness on hard ground can be used for traffic noise reduction. Effects may be improved by using resonant roughness. Various other methods employed to improve sonic crystal noise barrier performance (use of coupled resonances, vacancies and aperiodicity) are yet to be explored. For both outdoor sonic crystal noise barriers and designed ground effect, future studies will need to look at meteorological effects.

6 ACKNOWLEDGEMENTS

The research reported here has been supported by EPSRC grants GR/S35592, EP/H040617/1, EP/K03720X/1 and by EC FP7 HOSANNA Grant # 234306 www.greener-cities.eu.

7 REFERENCES

1. V.G.Veselago, Sov.Phys. Uspekhi **10**, 509-514 (1968).
2. A.Climente *et al*, Appl. Phys. Lett. **97**, 104103 (2010).
3. J.Li *et al*, Nature Mater. **8**, 931-934 (2009).
4. A.N.Norris, Proc.R.Soc. A **464**, 2411-2434 (2008)
5. V.V. Krylov, Acta Acust. united with Acust., **90**, 830-837 (2004)
6. V.V. Krylov and F.J.B.S. Tilman, J. Sound Vib. **274**, 605-619 (2004)
7. V.V. Krylov, and R.E.T.B. Winward, *J.Sound Vib.* **300**, 43-49 (2007)
8. Y.B.A. Chong, PhD Thesis, The Open University, 2010
9. O. Umnova *et al*, J. Acoust. Soc. Am. **119**, 278 - 284 (2006)
10. J. Sanchez-Dehesa *et al*, J. Acoust. Soc. Am. **129** 1173 - 1183 (2011)
11. M.S. Kushwaha and P. Halevi, J. Acoust. Soc. Am., **101**, 619-622 (1997)
12. E. Fuster-Garcia *et al*, Applied Physics Letter **90**, 244104 (2007).
13. A. Krynkin *et al*, J. Acoust. Soc. Am., **128**, 3496-3506 (2010)
14. D. P. Elford *et al*, J. Acoust. Soc. Am. **130** (5) 2746–2755 (2011)
15. A. Krynkin *et al*, J. Phys. D: Applied Physics, **44**, 125501 (2011)
16. V. Romero-Garcia, PhD Thesis, University Polytechnic of Valencia (2010)
17. D. Smirnov *et al*, Proc. IOA 40th meeting, NEC Birmingham (2014)
18. D. Cabellero et al, Phys. Rev. B, **64**:064303 (2001)
19. S. Castineira-Ibanez *et al* Archives of Acoustics **37** (4) 455–462 (2012)
20. ISO, *Acoustics—Attenuation of Sound During Propagation Outdoors—Part 2: A General Method of Calculation (ISO 9613-2)*. (ISO, Geneva, Switzerland, 1996)
21. S. Taherzaeh *et al*, J. Acoust. Soc. Am **123** (4) EL323-328 (2013)
22. I. Bashir, PhD Thesis, The Open University, 2014
23. T. v Renterghem *et al* J. Sound Vib. **331** 2404-2425 (2012)
24. T. v Renterghem *et al*, Proc. Euronoise, Prague 2012
25. B. vd Aa *et al*, Applied Acoustics, **74** (1) 89-101 (2013)
26. Garcia-Chocano *et al* Appl. Phys. Lett. **99** 074102 (2011)
27. V. V. Krylov *et al* unpublished report for the PEALS project (2014)
28. S. Brûlé *et al* Phys. Rev. Lett. **112**, 133901 (2014)
29. I. Bashir *et al*, J. Acoust. Soc. Am. **33** 1281 – 1292 (2013)
30. I. Bashir *et al* Applied Acoustics **83** 1-15 (2014)
31. H.-C. Shin *et al*, unpublished report for the PEALS project, 2014